Journal of Materials Chemistry B

Accepted Manuscript

ROYAL SOCIETY OF CHEMISTRY

www.rsc.org/materialsB

Journal Name

ARTICLE

TiO_2–B nanorods based competitive-like non-enzyme photoelectrochemical sensing platform for glucose noninvasive detection

Received 00th January 20xx,
Accepted 00th January 20xx

DOI: 10.1039/x0xx00000x

www.rsc.org/

Shupei Zhang[#a], Guifang Xu[#a], Lingshan Gong[a], Hong Dai[*a], Yilin Li[a], Zhensheng Hong[*b], Yanyu Lin[c]

TiO_2-B nanorods, with excellent performance including large specific surface area, open structure with significant voids, and continuous channels, were firstly explored in photoelectrochemical biosensing field. To reduce the destructive effect of UV light to biomolecules, dopamine was introduced onto TiO_2-B nanorods surface through coordinating dopamine with undercoordinated titanium atoms of TiO_2-B nanorods, which makes the complex promising matrix for subsequent biosensing. Furthermore, concanavalin A as recognition element was attached onto the TiO_2-B nanorods/dopamine modified electrode surface by virtue of covalent interaction between concanavalin A and dopamine. Accordingly, a new competitive-like non-enzyme photoelectrochemical biosensor was established by using glucose labeled SiO_2 nanospheres of fixed concentration as photoelectrochemical signal inhibitor competing with target glucose of various concentrations reacted with concanavalin A. Moreover, this ultrasensitive biosensor with excellent analytical performances was successful applied to the glucose noninvasive determination in humane saliva. Promising, the successful application of TiO_2-B nanorods in this research provides a new consideration for the selection of excellent photoactive materials in photoelectrochemical sensing.

1. Introduction

Photoelectrochemical (PEC) sensing, a newly emerged but dramatically progressed technique, is receiving increasing interest for sensing application because of its easy operation and simple instrument.[1] Furthermore, some undesired background signals could be reduced greatly due to the efficient separation of excitation sources (light) and detection signals (photocurrent) in the PEC detection process, leading to high sensitivity and good analytical performance.[2] Undeniably, photoconversion efficiency plays an actually vital role in the PEC detection sensitivity, which depends intimately on the photoactive materials immobilized on the substrate electrode.

From the materials perspective, TiO_2 is promising candidate for PEC sensing due to its high photoactivity, nontoxicity, superior stability, earth-abundance and cost efficiency.[3-4] Among various polymorphs of TiO_2, TiO_2-B, a metastable phase of titania, owns relatively more open structure with significant voids and continuous channels due to its perovskite-like layered structure and a slightly lower density, which makes it much higher charge-discharge capability and more excellent photoelectrical properties.[5-6] Therefore, TiO_2-B has drawn substantial attention in many fields including humidity rechargeable lithium ion batteries, dye-sensitized solar cells, photocatalytic cells, sensors and supercapacitors.[7-11] However, to date, no successful attempt has been demonstrated using TiO_2-B as a scaffold for PEC sensing. Herein, TiO_2-B nanorods (TiO_2-B NRs) synthesized by a simple and additive-free strategy under solvothermal (acetic acid) condition were used as photoactive specie to explore its PEC performance in biosensing.

Many efforts have been focused on the explorations of TiO_2-based photocatalysts to decrease the mismatch of the optical band gap with the entire solar spectrum.[12-13] Interestingly, enediol ligands were found that they had a large affinity for the undercoordinated surface Ti sites of TiO_2 species to form irreversible ligand-to-particle charge-transfer complexes, which makes the complex endow strong absorption ability in the visible light region.[14] Inspired by these, dopamine (DA) was introduced into this work. Herein, localized orbitals of surface attached ligands in DA were electronically coupled with the delocalized electron levels from the conduction band (CB) of TiO_2-B NRs, thus electrons can be excited under the illumination of visible light from the chelating ligands and then directly transfer into the CB of TiO_2-B NRs.[15] In addition, the complex with outstanding PEC performance and good biocompability can be used as a superior matrix to develop delicate PEC biosensors by using DA as a bridging linker.

Glucose, a small molecule, is the major energy source in human metabolism process. Furthermore, the concentration of glucose in

[a] College of Chemistry and Chemical Engineering, Fujian Normal University, Fuzhou, Fujian, 350108,China, Fax: (+86)-591-22866135,E-mail: dhong@fjnu.edu.cn
[b] Fujian Provincial Key Laboratory of Quantum Manipulation and New Energy Materials, College of Physics and Energy, Fujian Normal University, Fuzhou 350108, P. R. China, E-mail: winter0514@163.com
[c] Ministry of Education Key Laboratory of Analysis and Detection for Food Safety, and Department of Chemistry, Fuzhou University, Fuzhou 350002, P. R. China.
# These authors equally contributed to this work.
† Electronic Supplementary Information (ESI) available: See
DOI: 10.1039/x0xx00000x

blood is considered as a crucial indicator to the diagnosis of diabetes, one of the leading diseases causing disability and death for humans. Accordingly, it is much imperative to explore reliable strategy for glucose detection and many enzyme based biosensors have been fabricated because of its high selectivity and sensitivity.[16-17] To further expand the application scope, searching for enzyme-free sensor for glucose determination is of considerable interest.[18]

Herein, a sensitive non-enzymatic PEC biosensor was constructed based on TiO_2-B NRs/DA matrix for glucose detection by virtue of the high binding affinity between carbohydrate and Concanavalin A (ConA). ConA, a lectin protein with four saccharide bind sites extracted from the jack-bean, binds specifically to certain structures found in various sugars.[19-20] In addition, the amino group on lysine in ConA molecules affords a convenience for its immobilization onto other matrixs.[21] Therefore, ConA as a bionic recognition device anchored onto TiO_2-B NRs/DA surface to specifically determine glucose concentration by recording the decreased photocurrent. To further amplify the variable value of photocurrent, SiO_2 nanospheres (SiO_2 NSs), as signal-off labels, linked with glucose (SiO_2 NSs-glucose) competitive with target glucose for the specific recognition of ConA. Due to the large surface area, low toxicity, good stability and poor electroconductivity of SiO_2 NSs, the SiO_2 NSs-glucose can caused greater decrease value of photocurrent compared to that of glucose [22-23].

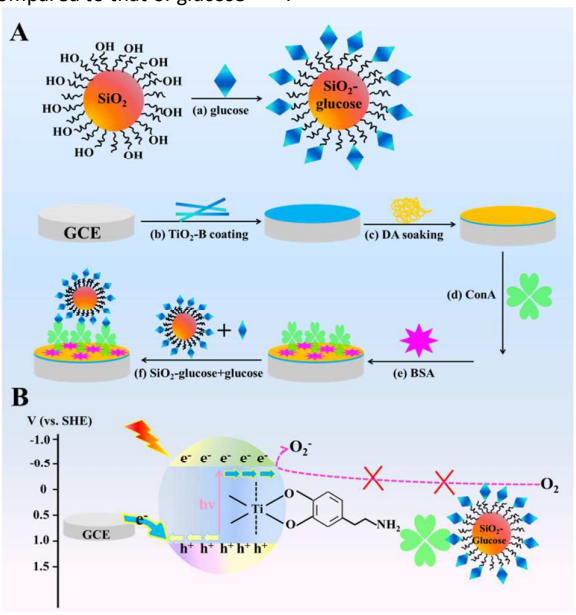

Scheme 1 (A) Schematic diagram of the competitive-like biosensor fabricates process. (B) Photocurrent generation mechanism of the PEC biosensor for glucose detection.

2. Experimental

2.1 Materials and Reagents

TiO_2 powder (P25) was obtained from the Degussa Co. (Germany). Acetic acid (HAc), Potassium hydroxide (KOH), Ammonium hydroxide, n-hexanol, Triton X-100 (TX-100), acetone, ethanol, cyclohexane, tetraethyl orthosilicate (TEOS) and glucose were purchased from Sinopham Chemical Reagent Co. (Shanghai, China). DA, glutaraldehtyde (GLD, 25% aqueous solution), ConA and bovine serum albumin (BSA, 96–99%) were purchased from Aladdin Industrial Corporation (Shanghai, China), Shanghai Jinshan Tingxin Chemical Plant (China), Shanghai yuanye Bio-Technology Co., Ltd (China) and Biss Inc. (Beijing, China), respectively. The phosphate buffer solution (PBS, 0.1 M, pH 7.4) as the supporting electrolyte was prepared by mixing stock solution of 0.1 M NaH_2PO_4 and 0.1 M Na_2HPO_4 and adjusting the pH. Deionized water (DI water) used for the preparation of the solution was purified using a Water purifier (China) purification system.

2.2 Apparatus

All the PEC measurements were performed with a homemade PEC system under 395 nm of irradiation. Photocurrents were record on a CHI 760 electrochemical workstation (Shanghai Chenhua Instrument Co., China) using a three-electrode system with a Ag/AgCl electrode (sat. KCl) reference electrode, a platinum wire as counter electrode and a modified glassy carbon electrode (3 mm in diameter) as working electrode. Scanning electron microscopy (SEM, S4800 instrument) and Transmission electron microscopy (TEM, FEI F20 S-TWIN instrument) were applied for the structural characterization of the products. X-ray diffraction (XRD) patterns were recorded on a PANalytical X'Pert spectrometer using the Co Kα radiation (λ = 1.78897 Å), and the data were changed to Cu Kα data.

2.3 Synthesis of TiO_2-B NRs, SiO_2 NSs and SiO_2 NSs-glucose conjugates

The TiO_2-B NRs were synthesized through solvothermal (HAc) method using titanate nanowires as precursors. Synthesis of titanate nanowires is similar with our previous work.[24] Typically, 1 g of TiO_2 was dispersed in a 75 mL of 15 M aqueous KOH solution. After stirring for 10 min, the resulting suspension was transferred into a 100 mL Teflon-lined stainless steel autoclave. The autoclave was kept at 170 ^{o}C for 72 h and then cooled to room temperature. The resulting precipitate was washed by diluted HAc solution until the pH was up to 7.0. The final product was then collected by centrifugation and dried at 60 ^{o}C for 12 h in air. Synthesis of TiO_2-B NRs started with dispersing 300 mg of precursor titanate nanowires 50 mL of 8 M HAc solution, and then transferred into a 100 mL Teflon-lined stainless steel autoclave, which was heated at 180 ^{o}C for 24 h. The final product was obtained by centrifuging and washing with distilled water and ethanol, dried at 60 ^{o}C overnight.

SiO_2 NSs were synthetized by a revised method in previous report.[25] Firstly, the mixed solution including 3.75 mL of cyclohexane, 885 μL of TX-100, 900 μL of n-hexanol and 170 μL of water was prepared. Then 30 μL of NH_4OH was added into the above mixture to initiate the polymerization reaction in the presence of 50 μL of TEOS. After the reaction was allowed to continue for 24 h under agitating, the product was isolated by acetone. Finally, the SiO_2 NSs were obtained by centrifugation and washed thoroughly with ethanol and water several times to remove any surfactant molecules, dried at 60 ^{o}C overnight.

SiO_2 NSs-glucose was prepared by mixing 500 μL of 1 mg mL^{-1} SiO_2 NSs and 500 μL of 10^{-5} mol L^{-1} glucose under sonicating for overnight at room temperature. Afterwards, the resulting mixture

was centrifuged at 10000r/min for 30 min to obtain the precipitate, and then added DI water to make final volume achieve 1 mL for subsequent application.

2.4 Fabrication of TiO_2-B NRs and TiO_2-B NRs/DA modified electrodes

Prior to modification, the bare glassy carbon electrode (GCE) was polished with 0.3 and 0.05 μm alumina slurry on chamois leather to produce a mirror-like surface, then it was washed successively with anhydrous alcohol and doubly distilled water in an ultrasonic bath and dried in air before use. With a micropipette, 4 μL of TiO_2-B NRs solution was dropped onto the fresh prepared GCE surface and dried at room temperature, which named as TiO_2-B NRs.

Subsequently, with a micropipette, 10 μL of 0.015M DA solution was dropped onto the TiO_2-B NRs modified electrode, and then it was put in dark for 20 min. Finally, the modified electrode was washed thoroughly with DI water to remove the DA of physical adsorption, which the modified electrode named TiO_2-B NRs/DA.

2.5 Construction of the PEC biosensor

The TiO_2-B NRs/DA was subsequently immersed into 60 μL of GLD solution for 50 min to active the NH_2- in DA and 60 μL of Con A (10^{-6} M) solution for 30 min to obtain TiO_2-B NRs/DA/ConA. Afterwards, the modified electrode was immersed into 60 μL of BSA (1 wt%) for 1 h to block possible active sites. Finally, the blocked TiO_2-B NRs/DA/ConA was sunk into the mixture including fixed concentration of SiO_2 NSs-glucose and different concentrations of target glucose at 4 ºC for 30 min. After each step, the electrode was washed thoroughly with DI water to remove the non-specificity absorption.

2.6 Preparation of saliva sample

Saliva samples were collected from healthy volunteers after rinsing their mouths with water. Subsequently, the samples were centrifuged at 2000 r/min for 30 min to obtain the supernatants and then stored at -20 ºC until analysis.

3. Results and Discussion

3.1 Structure characterizations of TiO_2-B NRs

To explore morphology and microstructure of TiO_2-B NRs, the SEM, TEM and HRTEM images were investigated in Figure 1. Obviously, large-scale monodisperse rods can be seen in Figure 1A. Besides, the nanorods structure with the length in the range of 45-60 nm can be further demonstrated from the low-resolution TEM image (Figure 1B). The corresponding SAED pattern form an area presented the lattice planes of (020), (110) and (310) in the inset of Figure 1B, which was well agreement with the monoclinic crystal structure of TiO_2-B. Furthermore, a well-crystallized structure with lattice fringes of about 0.62 nm was displayed in HRTEM image (Figure 1C), corresponding to the (001) plane of TiO_2-B. Remarkably, the width of the nanorods is tiny (around 7.5-8.5 nm), which is propitious to the fast transfer of electrons. Additionally, the phase structure and crystalline property of the nanorods were further investigated and analysed by the XRD pattern in Figure 1D. All the diffraction peaks can be indexed as monoclinic TiO_2-B phase (JCPDS 74-1940). The narrow sharp diffraction peaks at 2θ = 14.2°, 25.1°, 28.6°, and 48.6° can be well assigned to the (001), (110), (002), and (020) lattice planes of TiO_2-B, respectively, implying that high crystalline and only pure TiO_2-B formed in the products. The aforementioned findings clearly validated that the as-prepared material was a combination of nanorods morphology and TiO_2-B polymorph.

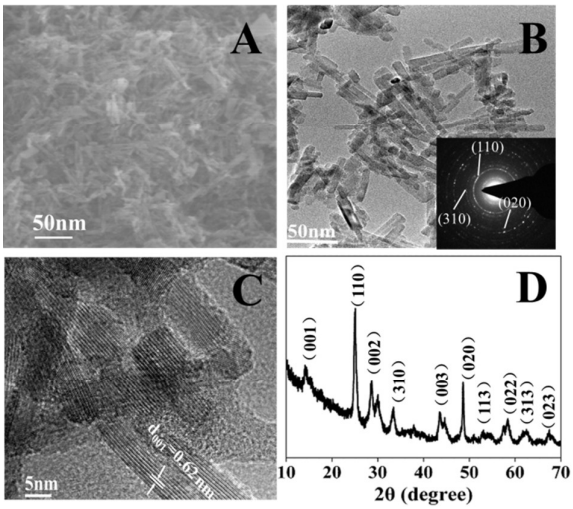

Figure 1 (A) SEM image, (B) TEM image, (C) HRTEM image and (D) XRD pattern of TiO_2-B NRs. The inset in (B) is a SAED pattern.

Besides, N_2 adsorption–desorption isotherms measurements (data not displayed) revealed that the TiO_2-B nanorods hold a large Brunauer-Emmett-Teller (BET) surface area (143 m^2 g^{-1}) and high pore volume (0.73 cm^3 g^{-1}), which provides a convenient for selective incorporation of various guest materials, effective interfacial charge collection and enhancement of light absorption.

3.2 Excellent PEC performance of TiO_2 –B NRs/DA

Although the significant voids and continuous channels of TiO_2-B NRs provide favourable conditions for its PEC application, wide band gap of TiO_2-B limit its absorption in visible region. Therefore, DA was introduced into this work in an attempt to enhance the PEC performance and photoelectric conversion efficiency. To certify the supposition, a series of PEC measurements were conducted. As depicted in Figure 2A, comparing with TiO_2-B NRs, TiO_2-B NRs/DA exhibited larger photocurrent density under all applied potentials, indicating TiO_2-B NRs/DA possessed better PEC performance.

Figure 2B displayed the typical open-circuit photovoltage (Voc) response under intermittent light illumination. Voc represents the difference in Fermi level between photoactive materials (in this work are TiO_2-B NRs and TiO_2-B NRs/DA) and counter electrodes. Under the light illumination, most of excited photoelectrons were collected within TiO_2-B NRs or TiO_2-B NRs/DA film, leading to the shift of the Fermi level to more negative potentials and the increase of Voc.[26-27] Therefore, Voc arrived to a steady state (maximum value) with the increasing photo-generated electrons in these thin-films under light illumination. Upon stopping the irradiation, Voc began to decay with the scavenging of accumulated photoelectrons by the electron acceptor species in the solution and the recombination with photoholes. As expected, TiO_2-B NRs/DA depicted a higher photovoltage under light illumination and slower decay in dark compared with TiO_2-B NRs, suggesting the more efficient charge

separation and less charge recombination for TiO_2-B NRs/DA complex, which was in good accordance with the result of Bode-phase plots in Figure 2C. The electron lifetime (τ_e) of photoactive material was calculated according to the following equation (1)[28]:

$$\tau_e = 1/2\pi f_{max} \quad (1)$$

Where f_{max} is the frequency at which the peak appears in the plot. Clearly, the TiO_2-B NRs/DA complex achieved an ms-scale lifetime (1.36 ms) that is about 23-fold slower than that of pure TiO_2-B NRs (60 μs). Unquestionably, the slower recombination will result in more opportunities for electron-hole separation.

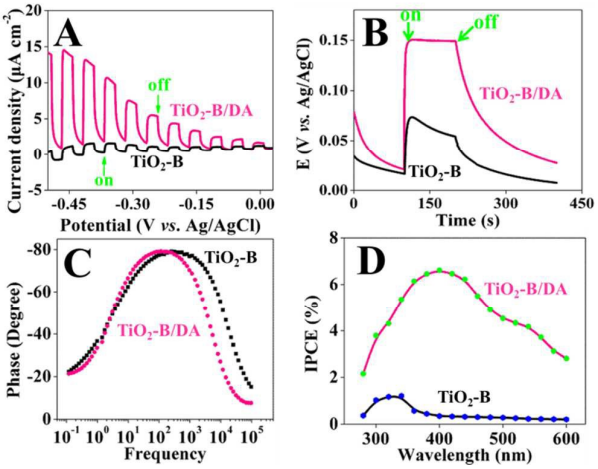

Figure 2 (A) Photocurrent densities-potential relationships under light on/off illumination, (B) Open-circuit photovoltage responses, (C) Bode-phase plots of TiO_2-B NRs and TiO_2-B NRs/DA in 0.5 M Na_2SO_4, (D) IPCE spectra of TiO_2-B NRs and TiO_2-B NRs/DA in 0.1 M PBS (pH 7.0).

Furthermore, incident photon-to-electron conversation efficiency (IPCE) spectra was investigated to further elucidate the effect of DA in Figure 2D. The IPCE values can be determined with no bias voltage based on equation (2)[27]:

$$IPCE\% = (1240 \times j \times 100)/(\lambda \times P) \quad (2)$$

where j is the measured photocurrent density in mA cm^{-2}, λ is the wavelength of the incident light in nm, P is the power intensity of the incident light at each wavelength in mW cm^{-2}. Notably, the photoresponse of pure TiO_2-B NRs in visible light region was minimal until the irradiation wavelength blue-shift to 380 nm, and then it sharply increased because of bandgap illumination reached. Expectedly, TiO_2-B NRs/DA complex exhibited enhanced photoresponse and higher IPCE value not only in UV but also in visible light region, which was resulted from the large energy shift of valence band in this complex. [14]

The aforementioned results are reasonable if taking into consideration of the synergic effect among improved charge separation, elongated electron lifetime, and enhanced light absorption. The results strongly confirmed that the introduction of DA indeed dramatically improved the PEC performance of TiO_2-B NRs. Accordingly, this complex with excellent photocatalytic performance was a promising candidate in PEC biosensing.

3.3 The tentative mechanism for the glucose detection

As a proof-of-concept application, a competitive-like enzyme-free PEC biosensor was developed in Scheme 1A and the tentative mechanism for glucose determination was proposed in Scheme 1B. In this work, ConA was connected to TiO_2-B NRs/DA modified electrode surface by means of GLD as a bridging linker. Subsequently, glucose was anchored onto electrode surface through the biospecific interactions between glucose and ConA, forming a like-immune complex. Due to the inhibition of this like-immune complex to the transfer of O_2, the photocurrent decreased. To further amplify the change of photocurrent signal, SiO_2 NSs-glucose competing with glucose to attached to ConA. Photocurrent density decreased with the decrease of glucose concentration because more and more SiO_2 NSs-glucose anchored onto modified electrode surface, which realized the ultrasensitive detection of glucose.

3.4 PEC biosensor characterization and detection strategy feasibility assay

To verify the above speculation, the stepwise fabricate process of this sensor was monitored in Figure 3A. In comparison with GCE (a), TiO_2-B NRs (b) presented a higher charge-transfer resistance (R_{ct}) due to poor electrical conductivity of TiO_2-B NRs, implying TiO_2-B NRs were successful dropped onto GCE. Obviously, the R_{ct} value reduced significantly after successful formation of DA-Ti complex (c) on electrode surface, which could be explained as that the positively charged DA in favor of the transfer of negatively charged $Fe(CN)_6^{3-/4-}$. As expected, R_{ct} value gradually increased after TiO_2-B NRs/DA (c) was soaked into ConA (d), the mixture of SiO_2 NSs-glucose and glucose (e) solution, which resulted from the nonconductive properties of ConA and SiO_2 NSs. The R_{ct} variation after each modification step provided the solid evidence for the successful construction of this biosensor.

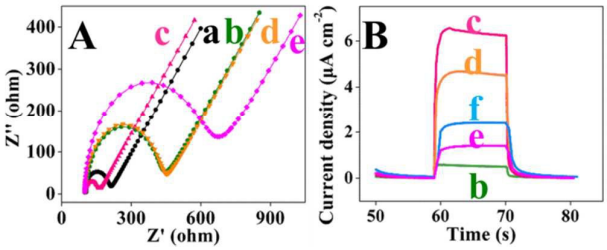

Figure 3 (A) Nyquist diagrams of EIS at different modified electrodes in 0.1 M KCl solution containing 5 mM $K_4[Fe(CN)_6]$/ $K_3[Fe(CN)_6]$. (B) Photocurrent responses at different modified electrodes in 0.1M PBS (pH 7.0) without biases voltage. GCE (a), TiO_2-B NRs(b), TiO_2-B NRs/DA (c), TiO_2-B NRs/DA/ConA (d), TiO_2-B NRs/DA/ConA incubation with 20 μL mixture containing 10 μL of SiO_2 NSs-glucose and 10 μL of 10^{-7} M (e) or 10^{-6} M(f) glucose.

The photocurrent densities of different modified electrodes were investigated to probe the feasibility of this biosensor in Figure 3B. As displayed in curve b, the TiO_2-B NRs demonstrated sensitive PEC response because of their large specific surface area and more open structure, which was propitious to the effective interfacial charge capture, enhanced light-scattering ability, and fast electrolyte diffusion. Expectedly, TiO_2-B NRs/DA (c) exhibited profound increased cathode photocurrent response (which can be proved in Figure S2) induced by the photoelectrons moved from the

chelating DA directly into the CB of TiO_2-B NRs. Subsequently, after the successful assembly of ConA (d) and SiO_2 NSs-glucose (e, f), the photocurrent density gradually decreased due to the steric hindrance of ConA and SiO_2 NSs. As exhibited in curve e and f, the photocurrent increased with the increase of glucose concentration. Based on the above investigates, we believe that the designed sensing strategy could be applied to determine glucose.

3.5 Analytical performance of the biosensor

Under the optimum conditions (Figure S3 and S4), the photocurrent densities of TiO_2-B NRs/DA/ConA after incubated in the mixture including fixed SiO_2 NSs-glucose concentration and various glucose concentrations were recorded to evaluate the detection performance of this biosensor. As manifested in Figure 4A, the photocurrent densities increased with the increase of target glucose concentration. In addition, the variation values of photocurrent density linearly increased with an increasing logarithm of glucose concentration in the range from 5×10^{-8} M to 10^{-3} M with a detection limit of 1.7×10^{-8} M (Figure 4B), which exceeded previous reports (Table S1).

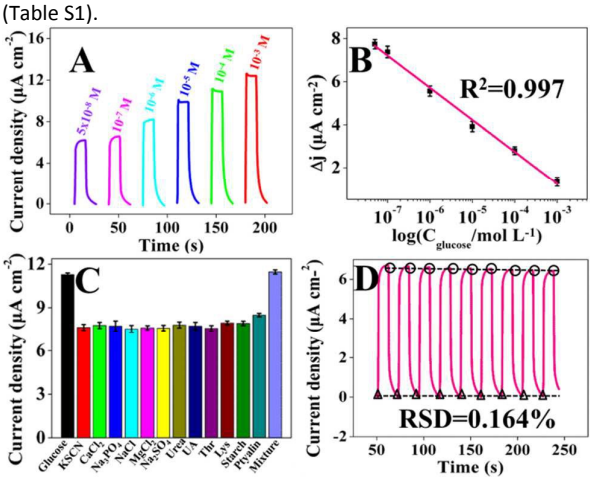

Figure 4 (A) The photocurrent densities for detection of different concentrations of target glucose. (B) The corresponding calibration curve. (C) The photocurrent densities of the prepared sensor to glucose with interfering substances. (D) The photocurrent response of the biosensor at10^{-7} M target glucose under repeat on/off cycles simulated light. 0.1 M PBS (pH 6.0), -0.2V.

To explore the specificity of this sensor, some potential interfering substances at an excess 20 folds concentration of glucose concentration were examined in Figure 4C. Obviously, the negligible change of photocurrent density was displayed, which clearly confirmed that this strategy possessed a reasonable selectivity towards glucose detection.

Furthermore, the stability and reproducibility of this biosensor are crucial for the practical applications. As provided in Figure 4D, not only the strong and stable photocurrents were observed in light illumination but also the positions of dark currents (zero) were not change, implying the excellent chemical and structural stability. Besides, there were no obvious photocurrent deteriorations after 15 days storage at 4 ºC, which indicated the biosensor owned good storage stability.

Additionally, reproducibility as an important criterion was investigated by testing five freshly fabricated modified electrodes. Under the same condition, the result manifested almost identical photocurrent with a RSD of 4.72 %, predicting the biosensor endowed good fabricate reproducibility.

To examine the applicability, the proposed competitive-like non-enzyme biosensor was used to detect glucose in human saliva (concentration of glucose in saliva is ca. 1% of that in blood). The results (Table S2) displayed that glucose concentration in the five healthy human were lower 80 μM, which was in good accordance with the results in previous reports.[29-30] In addition, the recovery of these five saliva samples was from 96.1% to 104.6%, demonstrating the designed biosensor can be used in the clinic application for ultrasensitive glucose determination in human saliva.

Conclusions

In summary, DA sensitized TiO_2-B NRs with outstanding PEC performance in visible light region and SiO_2 NSs with poor electroconductivity as matrix and signal-off labels, respectively, were used for the ultrasensitive glucose detection by means of the biospecific interaction between ConA and glucose. This biosensor displayed excellent analytical performance including wide linear range, high sensitivity, good specificity and robust stability. Especially, the wide linear range covered the glucose concentration not only in blood but also in saliva. Therefore, it provided a convenient condition for glucose noninvasive detection in human saliva, which eliminated pain, discomfort and superinfection originated from puncturing finger. Furthermore, the dissolved oxygen in the solution had a positive effect for the cathode photocurrent in PEC biosensing, which avoided the addition of supplementary substrates and the destructive effects of photo-generated holes to biomolecules. Unquestionably, this research not only depicts a successful paradigm for exploration of the fascinating properties of TiO_2-B NRs in its new application filed, but also paves a new channel for developing high performance PEC biosensor.

Acknowledgements

This project was financially supported by the NSFC (21205016), National Science Foundation of Fujian Province (2011J05020), Education Department of Fujian Province (JA14071, JB13008, JA13068), Fujian Normal University outstanding young teacher research fund projects (fjsdjk2012068) was also greatly acknowledged.

Notes and references

1 Y. T. Long, C. Kong, D.W. Li, Y. Li, S. Chowdhury and H. Tian, *Small*, 2011, **7**, 1624.
2 H. B. Li, J. Li, Q. Xu and X. Y. Hu, *Anal. Chem.*, 2011, **83**, 9681.
3 X. B. Chen, S. H. Shen, L. J. Guo and S. S. Mao, *Chem. Rev.*, 2010, **110**, 6503.

4 P. Hartmann, D. K. Lee, B. M. Smarsly and J. Janek, *ACS Nano*, 2010, **4**, 3147.
5 A. G. Dylla, G. Henkelman and K. J. Stevenson, *Acc. Chem. Res.*, 2013, **46**, 1104.
6 T. Kogure, T. Umezawa, Y. Kotani, A. Matsuda, M. Tatsumisago and T. Minami, *J. Am. Ceram. Soc.*, 1999, **82**, 3248.
7 A. R. Armstrong, G. Armstrong, J. Canales, R. Garcia and P. G. Bruce, *Adv. Mater.*, 2005, **17**, 862.
8 K. Asagoe, S. Ngamsinlapasathian, Y. Suzuki and S. Yoshikawa, *Cent. Eur. J. Chem.*, 2007, **5**, 605.
9 C. H. Lin, J. H. Chao, C. H. Liu, J. C. Chang and F. C. Wang, *Langmuir*, 2008, **24**, 9907.
10 G. Wang, Q. Wang, W. Lu and J. H. Li, *J. Phys. Chem. B*, 2006, **110**, 22029.
11 Q. Wang, Z. H. Wen and J. H. Li, *Adv. Funct. Mater.*, 2006, **16**, 2141.
12 P. Roy, C. Das, K. Lee, R. Hahn, T. Ruff, M. Moll and P. Schmuki, *J. Am. Chem. Soc.*, 2011, **133**, 5629**.**
13 X. Chen, L. Liu, P. Y. Yu and S. S. Mao, *Science*, 2011, **331**, 746.
14 T. Rajh, L. X. Chen, K. Lukas, T. Liu, M. C. Thurnauer and D. M. Tiede, *J. Phys. Chem. B*, 2002, **106**, 10543.
15 N. M. Dimitrijevic, Z. V. Saponjic, B. M. Rabatic and T. Rajh, *J. Am. Chem. Soc.*, 2005, **127**, 1344.
16 J. Wang, *Chem. Rev.*, 2008, **108**, 814.
17 C. Chen, Q. J. Xie, D. W. Yang, H. L. Xiao, Y. C. Fu, Y. M. Tan and S. Z. Yao, *RSC Adv.*, 2013, **3**, 4473.
18 T. W. Tsai, G. Heckert, L. F. Neves, Y. Tan, D. Y. Kao, R. G. Harrison, D. E. Resasco and D. W. Schmidtke, *Anal. Chem.*, 2009, **81**, 7917.
19 D. P. Tang, B. Zhang, J. Tang, H. Li and G.N. Chen, *Anal. Chem.*, 2013, **85**, 6958.
20 Z. H. Chen, Y. Liu, Y. Z. Wang, X. Zhao and J.H. Li, *Anal. Chem.*, 2013, **85**, 4431.
21 S. Q. Liu, K. W. Wang, D. Du, Y. M. Sun and L. He, *Biomacromolecules*, 2007, **8**, 2142.
22 M. Liong, J. Lu, M. Kovochich, T. Xia, S. G. Ruehm, A. E. Nel, F. Tamanoi and J. I. Zink, *ACS Nano*, 2008, **2**, 889.
23 J. Kim, H. S. Kim, N. Lee, T. Kim, H. Kim, T. Yu, I. C. Song, W. K. Moon and T. Hyeon, *Angew. Chem.*, 2008, **120**, 8566.
24 H. Dai, S. P. Zhang, L. S. Gong, Y. L. Li, G. F. Xu, Y.Y. Lin and Z. S. Hong, *Biosens. Bioelectron.*, 2015, **72**, 18.
25 S. Santra, P. Zhang, K. Wang, R. Tapec and W.H. Tan, *Anal. Chem.*, 2001, **73**, 4988.
26 B. H. Meekins and P. V. Kamat, *ACS Nano*, 2009, **3**, 3437.
27 X. M. Song, J. M. Wu, M. Z. Tang, B. Qi and M. Yan, *J. Phys. Chem. C*, 2008, **112**, 19484.
28 F. L. Gou, X. Jiang, B. Li, H. W. Jing and Z. P. Zhu, *ACS Appl. Mater. Interfaces*, 2013. **5**, 12631.
29 F. A. Wang, X. Q. Liu, C. H. Lu and I. Willner, *ACS Nano*, 2013. **7**, 7278.
30 D. X. Ye, G. H. Liang, H. X. Li, J. Luo, S. Zhang, H. Chen and J. L. Kong, *Talanta*, 2013, **116**, 223.

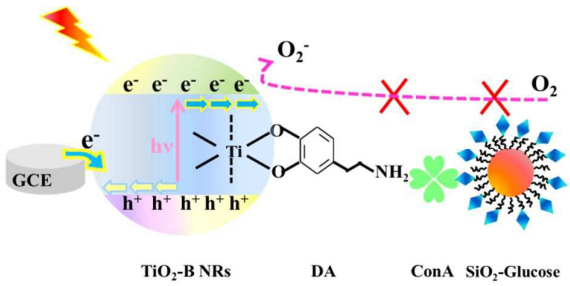

A new competitive-like non-enzyme photoelectrochemical biosensor was firstly established based on TiO_2–B nanorods platform for glucose noninvasive detection.